A Moment-Based Approach to Registration of Images with Affine Geometric Distortion

Jan Flusser and Tomáš Suk

Abstract—**This paper deals with the registration of images with affine geometric distortion. It describes a new method for automatic control point selection and matching. First, reference and sensed images are segmented and closed-boundary regions are extracted. Each region is represented by a set of affine-invariant moment-based features. Correspondence between the regions is then established by a two-stage matching algorithm that works both in the feature space and in the image space. Centers of gravity of corresponding regions are used as control points. A practical use of the proposed method is demonstrated by registration of SPOT and Landsat TM images. It is shown that our method can produce subpixel registration accuracy.**

Keywords—**image registration, affine geometric distortion, control points, affine moment invariants, region matching.**

I. Introduction

THE analysis of two or more digital images of the same scene taken from different places or at a different time often requires registration of the images.

Image registration is the process of overlaying two images of the same scene, one of which represents a reference image, while the other (called sensed image) is geometrically transformed. In remote sensing applications, this process is required in numerous tasks, for instance, in multitemporal classification, environmental monitoring, automatic change detection, and in map updating.

Image registration consists traditionally of three main steps:

- selection of control points (CP's) in the reference and sensed images and determination of the correspondence between them;
- determination of the type and parameters of the mapping functions using known coordinates of control points;
- geometric transformation of the sensed image by means of the mapping functions.

In this paper, a new method of control point selection is presented. This method is invariant under affine geometric distortion between reference and sensed images. In Section II, a brief review of the recent works is given. New affine-invariant region features are introduced in Section III. In Section IV, an algorithm for region matching is presented and the registration of two digital images of the Czech territory recorded by the SPOT HRV and Landsat TM sensors is shown.

Manuscript received September 17, 1992.

The authors are with the Institute of Information Theory and Automation, Czech Academy of Sciences, Pod vodárenskou věží 4, 18208 Prague 8, Czech Republic.

IEEE Log Number 9215453.

II. Control Point Selection

Automatic selection of control points is, in most cases, a two-stage process. The first step consists of the identification of significant points or structures in the images. In the second step, the mutual correspondence between the extracted structures is found (this step is called *image matching*).

Automatic control point selection has been the goal of ongoing research. There are two main approaches to solving this problem: *correlation-like* and *symbolic*.

A. Correlation-Like Methods

In this approach, the window centers are used as control points. The location of the window can be established by classical correlation [1], binary edge correlation [2], or vector correlation [3]. The correlation algorithm can be sped up by computing in Fourier domain [4], by the use of hierarchical image representation [5], or by sequential computing of window dissimilarity [6].

A common criticism of methods involving correlation techniques concerns their high computational complexity and sensitivity to rotation, scaling, and gray-level variations of the original images.

B. Symbolic Methods

Symbolic methods do not work directly with gray-level images. Instead, they use scene features such as line intersections, edges, and regions.

Stockman *et al.* [7] use line intersections as control points and determine the correspondence between them by means of cluster analysis. Zahn [8] and Stockman and Goshtasby [9] use graph matching for point correspondence determination.

Recently, several authors have proposed using the centers of gravity of closed-boundary regions as control points. This technique is very effective, namely, for following reasons:

- some closed-boundary regions can be found in almost every image (such regions can represent lakes, ponds, fields, forests, or urban areas);

- the property *to be the center of gravity* is invariant under rotation, scaling, and skewing;
- the coordinates of the center of gravity are very stable under random noise and gray-level variations in the original image (random noise affecting the region will average out and will have very little effect on the center of gravity).

There are several ways to establish the mutual correspondence between the regions: iterative probabilistic relaxation [10], logical tree classification [11], or feature-based classification.

In the feature-based classification, each region is described by its features, and region matching is performed in the feature space. Features of region description can include boundary descriptors [12], shape vector [13], shape matrix [14], Fourier descriptors [15], [16], or moment invariants [17]–[20].

C. Affine Geometric Distortion

All the above-mentioned methods can be used for the registration of images which differ only by a translation, rotation and scaling. The task we have to solve is to register images with *general affine distortion*. Affine distortion appears in remote sensing very often; it describes for example the image skew caused by Earth's rotation. Moreover, perspective projection is usually approximated by affine function (in the case of small nonlinear effects).

Formally, an affine relation between two images is described by the equations

$$u = a_0 + a_1 x + a_2 y$$
$$v = b_0 + b_1 x + b_2 y, \qquad (1)$$

where (x, y) and (u, v) are the coordinates in the reference and sensed images, respectively.

In this paper, we will use centers of gravity of closed-boundary regions as affine-insensitive control points. In order to establish the correspondence between the control points (i.e., between the regions), we have to find affine-invariant descriptors of the region shapes.

III. Affine Moment Invariants

The *affine moment invariants* (AMI's) are moment-based descriptors of planar shapes, which are invariant under general affine transformation (1). The AMI's were derived by means of classical theory of algebraic invariants (see [26], for instance). Full derivation and comprehensive discussion on the properties of invariants can be found in the recent paper by Flusser and Suk [21]. In this paper, we present only the most essential facts.

The central moment μ_{pq} of order $(p + q)$ of binary 2-D object G is defined as

$$\mu_{pq} = \int\int_G (x - x_t)^p (y - y_t)^q \, dx \, dy$$

where (x_t, y_t) are the coordinates of the center of gravity of object G.

The affine transformation (1) can be decomposed into six one-parameter transformations:

$$u = x + \alpha, \qquad u = \delta \cdot x,$$
$$v = y \qquad v = y$$
$$u = x, \qquad u = x + t \cdot y,$$
$$v = y + \beta \qquad v = y$$
$$u = \omega \cdot x, \qquad u = x,$$
$$v = \omega \cdot y \qquad v = t' \cdot x + y.$$

Any function $\mathfrak{F}$ of moments which is invariant under these six transformations will be invariant under the general affine transformation (1).

From the requirement of invariantness under these transformations, the type and parameters of the function $\mathfrak{F}$ can be found.

Four simplest AMI's that we have used in this paper for image registration are listed below in the explicit form:

$$I_1 = \frac{1}{\mu_{00}^4}(\mu_{20}\mu_{02} - \mu_{11}^2)$$

$$I_2 = \frac{1}{\mu_{00}^{10}}(\mu_{30}^2\mu_{03}^2 - 6\mu_{30}\mu_{21}\mu_{12}\mu_{03} + 4\mu_{30}\mu_{12}^3 + 4\mu_{03}\mu_{21}^3 - 3\mu_{21}^2\mu_{12}^2)$$

$$I_3 = \frac{1}{\mu_{00}^7}(\mu_{20}(\mu_{21}\mu_{03} - \mu_{12}^2) - \mu_{11}(\mu_{30}\mu_{03} - \mu_{21}\mu_{12}) + \mu_{02}(\mu_{30}\mu_{12} - \mu_{21}^2))$$

$$I_4 = \frac{1}{\mu_{00}^{11}}(\mu_{30}^3\mu_{03}^2 - 6\mu_{20}^2\mu_{11}\mu_{12}\mu_{03} - 6\mu_{20}^2\mu_{02}\mu_{21}\mu_{03} + 9\mu_{20}^2\mu_{02}\mu_{12}^2 + 12\mu_{20}\mu_{11}^2\mu_{21}\mu_{03} + 6\mu_{20}\mu_{11}\mu_{02}\mu_{30}\mu_{03} - 18\mu_{20}\mu_{11}\mu_{02}\mu_{21}\mu_{12} - 8\mu_{11}^3\mu_{30}\mu_{03} - 6\mu_{20}\mu_{02}^2\mu_{30}\mu_{12} + 9\mu_{20}\mu_{02}^2\mu_{21}^2 + 12\mu_{11}^2\mu_{02}\mu_{30}\mu_{12} - 6\mu_{11}\mu_{02}^2\mu_{30}\mu_{21} + \mu_{02}^3\mu_{30}^2).$$

The number of the invariants is dealt with in Cayley–Sylvester theorem [26]. It is proved in [21] that there is one invariant of weight 2 (I_1), one invariant of weight 4 (I_3), and two invariants of weight 6 (I_2 and I_4).

The invariants I_1–I_4 are composed only from central moments up to the third order. Zero-order moment μ_{00} is the area of object G. Second-order moments express the distribution of "matter" around the center of gravity. In the case of objects with mass, they are called *moments of inertia*. Third-order moments express the basic properties of symmetry of object G. They are equal to zero for objects with central symmetry.

Moments of higher order describe more slight variations in shape, but they are more sensitive to noise. For this reason, only moments up to the fourth order are suitable in practice. As we pointed out in [21], 27 independent invariants can be set up from fourth-order moments.

In our experience, the four AMI's I_1–I_4 are reliable enough for most practical tasks on remote sensing data matching. I_4 can be omitted in simple tasks. In some particularly complex tasks, when a lot of "similar" shapes are to be recognized, some of the simplest fourth-order invariants can be used, such as

$$I_5 = \frac{1}{\mu_{00}^6}(\mu_{40}\mu_{04} - 4\mu_{31}\mu_{13} + 3\mu_{22}^2)$$

and

$$I_6 = \frac{1}{\mu_{00}^9}(\mu_{40}\mu_{04}\mu_{22} + 2\mu_{31}\mu_{22}\mu_{13} - \mu_{40}\mu_{13}^2 - \mu_{04}\mu_{31}^2 - \mu_{22}^3).$$

IV. Numerical Experiment

To measure the performance of the proposed image registration method, the registration of multitemporal satellite images from SPOT HRV and Landsat TM sensors was carried out.

A. Data

In this experiment, two images of the district of Zlin (Czech Republic) were used.

The reference image was taken by SPOT in September 1987 (see Fig. 1). The sensed image was taken by Landsat TM in August 1988 (see Fig. 2). Subscenes of the size 512 × 512 pixels from the original images were used. Since both sensors produce multispectral images, only one spectral band was selected for the registration experiment (band 3 from SPOT and band 5 from Landsat TM images).

The geometric distortion between the reference and sensed images is approximately affine.

B. Region Extraction

In order to extract several closed-boundary regions, the following technique was used in the both images. (Note that our aim was not the full image segmentation, but only detection and extraction of regions with high contrast.)

First, each image was filtered by eight 3 × 3 Sobel masks to detect edges in various directions. The edge image was created as the maximum of those eight oriented-edge images. The edge image was binarized by low threshold (t = 40). After that, most of pixels were signed as "edge." In the binary image, closed-boundary regions were found. Only the regions having perimeters between 10 and 100 pixels were taken into account.

Finally, the region boundaries were refined by the contour-tracing technique in original images (not in the thresholded ones).

In this way, twelve regions from the SPOT image and fourteen regions from the Landsat TM image were extracted (see Figs. 3 and 4). The extracted regions represent mostly fields and ponds. However, there were some regions that appeared in only one of the images.

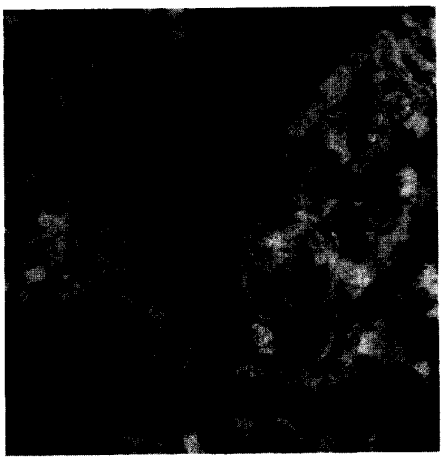

Fig. 1. The reference image—SPOT subscene, 512 × 512 pixels, band 3.

Fig. 2. The sensed image—Landsat TM subscene, 512-512 pixels, band 5.

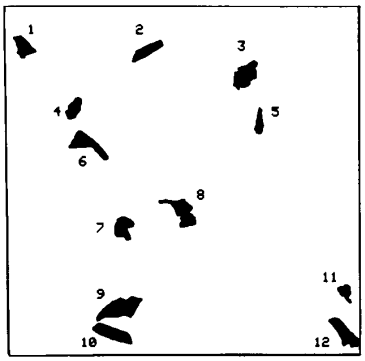

Fig. 3. Closed-boundary regions of the SPOT image.

C. Region Matching

The algorithm for region matching consists of two stages. The first stage is performed in the 4-D Euclidean feature space, the second one is performed in the image space.

Fig. 4. Closed-boundary regions of the Landsat TM image.

In the first stage, the local information about the regions represented by the AMI's is used to find three pairs of the most likely corresponding regions.

Let us denote S_i ($i = 1, \cdots, 12$) and T_j ($j = 1, \cdots, 14$) the regions in the SPOT and Landsat TM images, respectively. Let us denote ${}^{S}\mathrm{I}_1^{(i)}, \cdots, {}^{S}\mathrm{I}_4^{(i)}$ and ${}^{T}\mathrm{I}_1^{(j)}, \cdots, {}^{T}\mathrm{I}_4^{(j)}$ the values of the AMI's for the regions S_i and T_j, respectively.

For all i and j, we compute the feature distance d_{ij} between S_i and T_j:

$$d_{ij}^2 = \sum_{k=1}^{4} ({}^{S}\mathrm{I}_k^{(i)} - {}^{T}\mathrm{I}_k^{(j)})^2. \tag{2}$$

Now the minimum distance classification can be performed: we find indexes i_0, j_0, i_1, j_1, i_2, and j_2 such that

$$\begin{aligned} d_{i_0 j_0} &= \min_{i,j} d_{ij} \\ d_{i_1 j_1} &= \min_{\substack{i \neq i_0 \\ j \neq j_0}} d_{ij} \\ d_{i_2 j_2} &= \min_{\substack{i \neq i_0, i_1 \\ j \neq j_0, j_1}} d_{ij}. \end{aligned} \tag{3}$$

In this way, three corresponding pairs of the regions are determined: $S_{i_0} \approx T_{j_0}$, $S_{i_1} \approx T_{j_1}$, and $S_{i_2} \approx T_{j_2}$.

In the second stage, having three pairs of CP's (the centers of gravity of the regions S_{i_0}, T_{j_0}, S_{i_1}, T_{j_1}, S_{i_2}, and T_{j_2}), the parameters of the affine distortion (1) can be simply calculated. Knowing them, we can map the other region of the sensed image into the reference image. Region-to-region correspondence is then established by nearest neighbor rule. However, some rejection threshold must be applied to avoid false match.

More formally, the whole algorithm can be described as follows.

Algorithm MATCH:

1. Denote $S_1, \cdots, S_N$ the regions in the first image, and $T_1, \cdots, T_M$ the regions in the second one.
2. Construct two point sets

   $\mathfrak{S} = \{(x_i, y_i) | x_i, y_i$ are coordinates of the center of gravity of region $S_i\}$,

   $\mathfrak{T} = \{(u_j, v_j) | u_j, v_j$ are coordinates of the center of gravity of region $T_j\}$.
3. Compute the $N \times M$ matrix D with elements d_{ij} given by (2).
4. Find indexes i_0, j_0, i_1, j_1, i_2, and j_2 defined by relations (3).
5. Solve the following system of linear equations with variables a_0, a_1, a_2, b_0, b_1, and b_2:

$$\begin{aligned} u_{j_0} &= a_0 + a_1 x_{i_0} + a_2 y_{i_0} \\ v_{j_0} &= b_0 + b_1 x_{i_0} + b_2 y_{i_0} \\ u_{j_1} &= a_0 + a_1 x_{i_1} + a_2 y_{i_1} \\ v_{j_1} &= b_0 + b_1 x_{i_1} + b_2 y_{i_1} \\ u_{j_2} &= a_0 + a_1 x_{i_2} + a_2 y_{i_2} \\ v_{j_2} &= b_0 + b_1 x_{i_2} + b_2 y_{i_2}. \end{aligned}$$

6. Define the distance threshold $r > 0$. For $i = 1, \cdots, N$ compute

$$\begin{aligned} u &= a_0 + a_1 x_i + a_2 y_i \\ v &= b_0 + b_1 x_i + b_2 y_i. \end{aligned}$$

   Let $(u_j, v_j) \in \mathfrak{T}$ be the closest point to (u, v). If

$$(u - u_j)^2 + (v - v_j)^2 < r^2$$

   then S_i and T_j correspond with each other. If not, region S_i is marked to have no corresponding region in the second image.

In our experiment, the following pairs of regions were found after the first stage of the matching algorithm: $7 \approx K$, $2 \approx E$, and $6 \approx J$. The complete matching results determined after the second stage are summarized in Table I.

What is the robustness of the presented matching algorithm? The first stage of algorithm *MATCH* (i.e., steps 1–4) may generate a false match in some particular cases. If all regions have very similar shapes, their AMI values are close to each other and the regions are not well separated in the feature space. The matching results may be then significantly affected by small noise. Similar problems appear if the region boundaries are corrupted by noise or by inaccurate segmentation. However, in such situations, almost every feature-based region matching procedure will fail.

In order to avoid mismatch in the first stage, a more robust but more computationally expensive method which uses so-called *matching likelihood coefficients* [27] can be applied. Matching likelihood coefficients are calculated from matrix D and express the reliability of matching for each possible pair of regions.

TABLE I
CORRESPONDENCE BETWEEN THE REGIONS OF THE SPOT AND LANDSAT TM IMAGES

SPOT	1	2	5	6	7	8	9	11
TM	D	E	I	J	K	L	M	N

TABLE II
COORDINATES OF CORRESPONDING CONTROL POINTS

Control Point	SPOT		TM		Produced by Regions
	x[pix]	y[pix]	u[pix]	v[pix]	
1	28.7	60.8	98.6	246.8	1 D
2	206.9	66.0	218.9	245.7	2 E
3	365.6	170.4	325.6	309.9	5 I
4	119.6	201.8	164.5	338.6	6 J
5	170.0	322.3	201.1	416.9	7 K
6	254.3	299.5	255.5	399.5	8 L
7	164.7	439.9	200.7	495.9	9 M
8	489.2	416.8	416.3	470.9	11 N

The second stage (i.e., steps 5 and 6) is very robust and it cannot fail, if the first part has produced a correct match.

However, if less than three closed-boundary regions have been detected in one of the images or if less than three corresponding pairs have been found in the first stage, algorithm *Match* is inapplicable.

D. Control Point Selection

Centers of gravity of corresponding regions were used as control points. In this way, eight pairs of control points were obtained. Since the determination of parameters of the affine transformation (1) requires knowledge of at least three control points, this number is sufficient.

In the case of inaccurate initial segmentation of the original images, the region refinement technique by Goshtasby *et al.* [22] can be modified for affine distortion and for the use of the AMI's, and can be applied to each pair of corresponding regions in order to refine the control point coordinates. In our experiment, the use of the refinement technique was not necessary.

Coordinates of all control points are shown in Table II.

E. Mapping Function Determination

Given a number of corresponding control points in two images, in this section we estimate the parameters of the mapping functions.

According to the presumption on the affine character of distortion, the mapping functions $u = u(x, y)$ and $v = v(x, y)$ must have the form (1).

Having more than three control points, we use the least squares technique to compute parameters a_0, a_1, a_2, b_0, b_1, and b_2.

If the presumption on the affine character of distortion does not hold exactly, we have to use more complex mapping functions instead of (1). Thin-plate splines [23], [25] or adaptive mapping functions [24] are appropriate in that case.

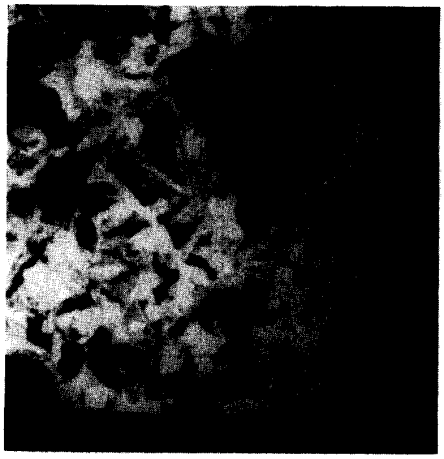

Fig. 5. The Landsat TM image after geometric transformation.

TABLE III
SQUARE ROOT ERRORS AT THE CONTROL POINTS

CP	1	2	3	4	5	6	7	8
err 1	0.7	1.1	0.9	0.7	0.4	0.8	0.2	0.4
err 2	1.6	0	1.9	0.2	0.5	1.0	0	0

F. Transformation of the Sensed Image

Knowing coefficients of the mapping functions (1), we can transform the Landsat TM image pixel by pixel. The result of transformation is shown in Fig. 5. Bilinear resampling of the sensed image was used for gray-level interpolation.

G. Registration Accuracy

To determine the accuracy of the registration, the square root errors were computed for each of the 8 pairs of CP's. Most errors are less than 1 pixel, and the mean is only 0.7 pixels. However, error computing at the CP's which were used for transformation parameters estimation might lead to too optimistic claims, because the least square technique optimizes the error at CP's.

To avoid such false claims, a more rigorous accuracy test was performed. Only three CP's were used to determine the registration parameters (CP's 2, 7, and 8; see Table II). The other CP's were used for error calculation only. The square root errors are a little bit larger than in the previous case, but only two of them are greater than 1 pixel.

The square root errors are summarized in Table III—err_1 denotes the errors in the first test, err_2 denotes the errors in the second one.

V. CONCLUSION

This paper has dealt with the registration of two images of the same scene with an affine geometric distortion. This requirement appears very often in the processing of multitemporal satellite images.

Attention has been paid to the automatic control point selection. First, the images are segmented by standard techniques, and closed-boundary regions are extracted. This paper describes a new method for the determination of corresponding regions. Each region is represented by affine moment invariants that are affine-invariant features describing the shape of the region. Region matching is then implemented as a two-stage process. The first stage consists of classification in Euclidean feature space; in the second stage, the region-to-region correspondence is established by the nearest neighbor rule in the image space.

After the correspondence between the regions has been established, centers of gravity of the corresponding regions are used as control points. The parameters of affine mapping functions are computed by the least square rule, and the sensed image is resampled and overlayed over the reference one.

The performance of the proposed algorithm has been demonstrated by registration of SPOT and Landsat TM images taken in different years. Subpixel registration accuracy has been reached in this experiment.

The presented method has been shown to be suitable for automatic registration of images with affine geometric distortion. However, our method is inapplicable or could lead to misregistration in some particular situations:

- initial segmentation of the images is very poor, and regions with false boundaries are extracted;;
- less than three closed-boundary regions are found in one of the images;
- there are not at least three pairs of corresponding regions among the extracted regions;
- extracted regions are not distinguishable by the AMI's (they have approximately the same shape).

The proposed approach to image registration may have numerous applications in aerial and satellite remote sensing for automatic environmental change detection, monitoring, and multitemporal classification.

References

[1] W. K. Pratt, "Correlation techniques of image registration," *IEEE Trans. Aerosp. Electron. Syst.*, vol. AES-10, pp. 353–358, 1974.

[2] P. Van Wie and M. Stein, "A Landsat digital image rectification system," *IEEE Trans. Geosci. Electron.*, vol. GE-15, pp. 130–137, 1977.

[3] J. S. Boland and H. S. Ranganath, "Automatic handoff of multiple targets," Tech. Rep., Auburn, Univ., AL, 1980.

[4] P. E. Anuta, "Spatial registration of multispectral and multitemporal digital imagery using FFT techniques," *IEEE Trans. Geosci. Electron.*, vol. GE-8, pp. 353–368, 1970.

[5] R. Y. Wong and E. L. Hall, "Sequential hierarchical scene matching," *IEEE Trans. Comput.*, vol. C-27, pp. 359–366, 1978.

[6] D. I. Barnea and H. F. Silverman, "A class of algorithms for fast digital image registration," *IEEE Trans. Comput.*, vol. C-21, pp. 179–186, 1972.

[7] G. C. Stockman, S. Kopstein, and S. Benett, "Matching images to models for registration and object detection via clustering," *IEEE Trans. Pattern Anal. Mach. Intell.*, vol. PAMI-4, pp. 229–241, 1982.

[8] C. T. Zahn, "An algorithm for noisy template matching," in *Proc. IFIP Cong.*, Stockholm, Sweden, 1974, pp. 698–701.

[9] A. Goshtasby and G. C. Stockman, "Point pattern matching using convex hull edges," *IEEE Trans. Syst., Man, Cybern.*, vol. SMC-15, pp. 631–637, 1985.

[10] J. Ton and A. K. Jain, "Registering Landsat images by point matching," *IEEE Trans. Geosci. Remote Sensing*, vol. GE-27, pp. 642–651, 1989.

[11] A. D. Ventura, A Rampini, and R. Schettini, "Image registration by recognition of corresponding structures," *IEEE Trans. Geosci. Remote Sensing*, vol. GE-28, pp. 305–314, 1990.

[12] T. Pavlidis, "A review of algorithms for shape analysis," *Comput. Graph. Image Processing*, vol. 7, pp. 243–258, 1978.

[13] T. Peli, "An algorithm for recognition and localization of rotated and scaled objects," *Proc. IEEE*, vol. 69, pp. 483–485, 1981.

[14] J. Flusser, "Invariant shape description and measure of object similarity," in *Proc. 4th Int. Conf. Image Processing*, Maastricht, The Netherlands, 1992, pp. 139–142.

[15] C. C. Lin and R. Chellappa, "Classification of partial 2-D shapes using Fourier descriptors," *IEEE Trans. Pattern Anal. Mach. Intell.*, vol. PAMI-9, pp. 686–690, 1987.

[16] N. Kiryati, "Calculating geometric properties of objects represented by Fourier coefficients," in *Proc. CVPR '88*, Ann Arbor, MI, 1988, pp. 641–646.

[17] M. K. Hu, "Visual pattern recognition by moment invariants," *IRE Trans. Inform. Theory*, vol. IT-8, pp. 179–187, 1962.

[18] S. Maitra, "Moment invariants," *Proc. IEEE*, vol. 67, pp. 697–699, 1979.

[19] T. C. Hsia, "A note on invariant moments in image processing," *IEEE Trans. Syst., Man, Cybern.*, vol. SMC-11, pp. 831–834, 1981.

[20] R. Y. Won and E. L. Hall, "Scene matching with invariant moments," *Comput. Graph. Image Processing*, vol. 8, pp. 16–24, 1978.

[21] J. Flusser and T. Suk, "Pattern recognition by affine moment invariants," *Pattern Recognition*, vol. 26, pp. 167–174, 1993.

[22] A. Goshtasby, G. C. Stockman, and C. V. Page, "A region-based approach to digital image registration with subpixel accuracy," *IEEE Trans. Geosci. Remote Sensing*, vol. GE-24, pp. 390–399, 1986.

[23] A. Goshtasby, "Registration of images with geometric distortions," *IEEE Trans. Geosci. Remote Sensing*, vol. GE-26, pp. 60–64, 1988.

[24] J. Flusser, "An adaptive method for image registration," *Pattern Recognition*, vol. 25, pp. 45–54, 1992.

[25] M. J. Baker, R. J. Beatson, R. Frick, and G. N. Newsam, "A fast algorithm for registering images using thin plate smoothing splines," in *Proc. 6th Australasian Remote Sensing Conf.*, vol. III, Wellington, New Zealand, 1992, pp. 11–20.

[26] I. Schur, *Vorlesungen uber Invariantentheorie*. Berlin: Springer, 1968 (in German).

[27] J. Flusser, "A feature-based approach to image matching," in *Computer Analysis of Images and Patterns*, R. Klette, Ed. Berlin: Akademie Verlag, 1991.

Jan Flusser was born in Prague, Czech Republic, on April 30, 1962. He received the M.Sc. degree in mathematical engineering from the Czech Technical University, Prague, Czech Republic in 1985 and the Ph.D. degree in computer science from the Czechoslovak Academy of Sciences in 1990.

Since 1985 he has been employed by the Institute of Information Theory and Automation, Czech Academy of Sciences, Prague. Since 1992 he has been a lecturer in Digital Image Processing at the Faculty of Mathematics and Physics, Charles University, Prague.

His current research interests include digital image processing, pattern recognition and remote sensing.

Tomáš Suk was born in Prague, Czechoslovakia, on April 30, 1964. He received the M.Sc. degree in electrical engineering from Czech Technical University of Prague, Czechoslovakia, in 1987 and the Ph.D. degree from Czechoslovak Academy of Sciences, in 1992.

His research interests include digital image processing and remote sensing.